


A comparative metabolomic investigation of different sections of Sicilian *Citrus x limon* (L.) Osbeck, characterization of bioactive metabolites, and evaluation of in vivo toxicity on zebrafish embryo

Stefania Pagliari¹ | Mirea Sicari³ | Lidia Pansera³ | Werther Guidi Nissim¹  | Kamel Mhalhel³ | Sepand Rastegar⁴ | Antonino Germanà³ | Nicola Cicero^{3,5,6} | Massimo Labra^{1,2} | Ciro Cannavacciuolo¹ | Giuseppe Montalbano³ | Luca Campone^{1,2}

¹Department of Biotechnology and Biosciences, University of Milano-Bicocca, Milan, Italy

²NBFC, National Biodiversity Future Center, Palermo, Italy

³Zebrafish Neuromorphology Lab, Department of Veterinary Sciences, University of Messina, Messina, Italy

⁴Institute of Biological and Chemical Systems—Biological Information Processing (IBCS-BIP), Karlsruhe Institute of Technology, Karlsruhe, Germany

⁵Department of Biomedical and Dental Science and Morphofunctional Imaging, University of Messina, Messina, Italy

⁶Science4life Spin-off Company, University of Messina, Messina, Italy

Correspondence

Ciro Cannavacciuolo, Department of Biotechnology and Biosciences, University of Milano-Bicocca, Milan, Italy.
Email: ciro.cannavacciuolo@unimib.it

Abstract: Citrus fruits are a diverse and economically important group of fruit crops known for their distinctive flavors and high nutritional value. Their cultivation and consumption contribute significantly to the global agricultural economy and offer a wide range of health benefits. Among the genetic diversity of citrus species, *Citrus x limon* (L.) Osbeck is particularly relevant due to its chemical composition and potential health benefits. Two cultivars from the Sicily region (southern Italy) were compared for their phenolic content and preliminary antioxidant activity to select the distinctive extract with potential biological activity. A detailed characterization revealed the occurrence of phenolics, coumarins, and flavonoids. The quantification of metabolites contained in the selected extract was performed by an ultrahigh-performance liquid chromatographic method coupled with an ultraviolet detector. Different concentrations were tested in vivo through the fish embryo acute toxicity test, and the 50% lethal dose of 107,833 $\mu\text{g mL}^{-1}$ was calculated. Finally, the effect of the extract on hatching was evaluated, and a dose-dependent relationship with the accelerated hatching rate was reported, suggesting a Femminello Zagara Bianca green peel upregulating effect on the hatching enzymes.

KEYWORDS

metabolomic, zebrafish, multivariate analysis, mass spectrometry, antioxidant activity

Giuseppe Montalbano, Zebrafish
Neuromorphology Lab, Department of
Veterinary Sciences, University of
Messina, 98168 Messina, Italy.
Email: giuseppe.montalbano@unime.it

Funding information

The Regional Department of Agriculture,
Rural Development and Mediterranean
Fisheries of the Sicily Region, Italy PO
FEAMP SICILIA 2014/2020—Project:
INNOVITICA, Grant/Award Number:
G35F20006240009; National Recovery and
Resilience Plan (NRRP), Mission 4
Component 2 Investment 1.3—Call for
tender No. 341 of 15 March 2022 of Italian
Ministry of University and Research
funded by the European
Union—NextGenerationEU; Award
Number: Codice progetto PE000000003,
Decreto Direttoriale MUR n. 1550 dell'11
ottobre 2022 di concessione del
finanziamento, CUP D93C22000890001,
titolo progetto “ON Foods—Research and
innovation network on food and nutrition
Sustainability, Safety and
Security—Working

Practical Application: Citrus fruits and their products continue to be one of the natural food sources with the highest waste output. In this study, we demonstrate how food industry waste, particularly lemon peel, is rich in bioactive compounds with anti-inflammatory and antioxidant properties that may be used in the nutraceuticals industry.

1 INTRODUCTION

The *Citrus* genus has an economic impact on the food chain and botanical production with an annual production of approximately 143.48 million tons (Nieto et al., 2021). *Citrus x limon* (L.) Osbeck, grown in the Mediterranean Area in specific areas of southern Italy (e.g., Sicily). In particular, the “Femminello Siracusano” (FS) and “Femminello Zagara Bianca” (FZB) are protected by the label “protected geographical indication” and represent the main cultivars produced in the Siracusa area. Although both varieties are considered different on a genetic basis (Guardo et al., 2021), the Femminello group, which includes both varieties, shows some common morphophysiological traits, including an ever-blooming, ever-bearing habit that makes these two varieties very responsive to the forced summer production of Sicilian lemon culture. However, although FS is the widely planted lemon variety in Italy during the past decade, showing outstanding performances in terms of productivity, yield precocity, and fruit quality, “Femminello Zagara Bianca” must be preferred in areas of high mal secco pressure (Barry et al., 2020). After processing, citrus byproducts still contain high-value compounds, such as dietary fiber, terpenes, phenolic acid, and polyphenol (Gómez-Mejía et al., 2019; Imeneo et al., 2022), which are largely used in nutraceuticals and cosmetic industries (Berk, 2016). Polyphenols play many biological roles, such as decreasing the expression of

some inflammatory mediators in vitro and in vivo (Cirmi et al., 2021; de Souza et al., 2022) and reducing oxidative stress (Bussmann et al., 2022; Montalbano et al., 2021-a). Thus, they prevent pathological processes such as aging and age-related diseases (Burton et al., 2016; Yousefzadeh et al., 2018), cancer (Tuli et al., 2023), obesity (Montalbano et al., 2019, 2021-b), and cardiovascular diseases (Liu et al., 2022-a). Furthermore, they have attracted great interest in contrasting neurodegenerative disorders due to their anti-apoptotic mechanisms and enhancing neuronal plasticity (Mhalhel et al., 2023). Zebrafish (*Danio rerio*), a small fish belonging to the Cyprinidae family, has recently emerged as a powerful vertebrate model in the fields of environmental toxicology assessment (Stegeman et al., 2010) and drug discovery (Cassar et al., 2019; Chakraborty et al., 2009) due to its affordability, sensitivity, and adaptability. The zebrafish embryo's transparency makes it possible to observe embryonic development and allows for noninvasive examination of organ development and toxic endpoints. These characteristics allow for the testing of very large chemical libraries with hundreds of thousands of compounds for drug discovery, leading to new therapeutics and the development of new research reagent tools using high-throughput screening (HTS) techniques (Letamendia et al., 2012). In line with highly bioactive properties reported for *Citrus*, this study aimed to compare the phenolic profiles of FS and FZB cultivars harvested in Sicily. Different fruit parts (i.e., peel,

pulp, seeds, and albedo) at two different ripening stages (i.e., green and yellow lemons) were considered to select the best part of the fruit and ripening stage, providing the higher recovery of the phenolic fraction with biological activities. The screening of all the hydroalcoholic extracts, aimed at selecting the extract with a higher phenolic content and a promising biological activity, was performed by the determination of total polyphenol content (TPC) and related capacity to quench DPPH and ABTS radicals evaluated by spectrophotometric assays. Once the detailed characterization by ultrahigh-performance liquid chromatography–ultraviolet/high-resolution mass spectrometry/MS (UHPLC-UV/HRMS/MS) analysis and the evaluation of the preliminary antioxidant assays were evaluated, a metabolomic approach by multivariate data analysis was carried out with principal component analysis (PCA) and supervised partial least squares (PLS) projection techniques to have a general overview of all the complex datasets and select the peels in the early ripening stage (green lemon) of FZB as representative for its higher phenol content, complex chemical profile, and preliminary antioxidant capacity. The selected extract was considered for further quantitative and in vivo investigations. In particular, the semiquantitative analysis of the most representative secondary metabolites occurring in the selected extract was evaluated by UHPLC-UV, and the extract was submitted to an in vivo toxicity assay on zebrafish embryo using the fish embryo acute toxicity test (FET; OECD TG 236) (Organisation for Economic Co-operation and Development [OECD], 2013).

2 | MATERIALS AND METHODS

2.1 | Chemical and reagents

MS-grade acetonitrile (ACN) and water were supplied by Romil (Cambridge). Ultrapure water (18 M Ω) was prepared by a Milli-Q purification system (Millipore). Analytical-grade methanol (MeOH) and ethanol (EtOH), MS-grade formic acid (HCOOH) were supplied by Sigma-Aldrich. Standards of hesperetin ($\geq 98\%$ HPLC), luteolin ($\geq 98\%$ HPLC), eriocitrin ($\geq 98\%$ HPLC), rutin ($\geq 98\%$ HPLC), apigenin ($\geq 98\%$ HPLC), naringenin ($\geq 98\%$ HPLC), and coumarin ($\geq 98\%$ HPLC) were obtained from Sigma-Aldrich.

2.2 | Sample collection

The two different Sicilian cultivars of *Citrus limon* FS and FZB, were provided by “Vasile Sebastiano farm” (Siracusa). Samples were collected at two different stages of ripeness in the October and November periods (i.e., green

and yellow stages). All lemons were grown under equal agronomic and environmental conditions. After the collection of the samples, they were stored at +4°C for one night.

2.3 | Extraction and sample preparation

Hydroalcoholic extraction of all parts (peel, pulp, seeds, and albedo) of the lemon of both FS and FZB cultivars was performed as reported in our paper with slight modification (Cannavacciuolo et al., 2023). The matrices were dried in an oven at a controlled temperature of 40°C; throughout the drying process, a digital balance (Sartorius Weighing Technology, GmbH) was used to record the weight change until all samples reached an unchanged weight evolution to the respective part (2–4 days) and then were reduced to powder by mechanical grinding. For each powder, 250 mg was weighed, and 5 mL of a solution of EtOH-H₂O (50% v/v) was added. The ultrasonic bath was set at room temperature, and three cycles of sonication were performed for a time of 10 min. The supernatants were recovered by centrifugation at 6000 rpm for 5 min. The supernatants obtained from the three cycles (15 mL) were transferred to a glass flask, and the organic solvent was removed via Rotavapor. The aqueous samples were stored at –80°C overnight and then subjected to freeze-drying until the dry extract was obtained.

2.4 | Determination of total phenol content

Determination of the total phenolic content (TPC) of the individual parts of each cultivar at the two different stages of ripening was carried out according to the Folin–Ciocalteu method using gallic acid as the calibration standard (D’Urso et al., 2020). Briefly, 20 μ L of diluted extract (0.3 mg mL^{–1}) and 5 μ L of Folin–Ciocalteu reagent were diluted with 145 μ L of reagent water and mixed with 30 μ L of Na₂CO₃ (20% v/v) in a 96-well microplate. After 45 min at 25°C, absorbance was read at 765 nm with a Multiskan GO spectrophotometer (Thermo Fisher Scientific). Results were expressed as mg of gallic acid equivalent (GAE) contained in 1 g of dry matrix (mg GAE g^{–1} DW) obtained by the mean of three independent measurements considering the standard deviation (SD) (Figure 1A).

2.5 | Measurement of antioxidant capacity (ABTS and DPPH assays)

The radical scavenging activity of extracts was determined using the 1,1-diphenyl-2-picrylhydrazyl radical (DPPH \cdot)

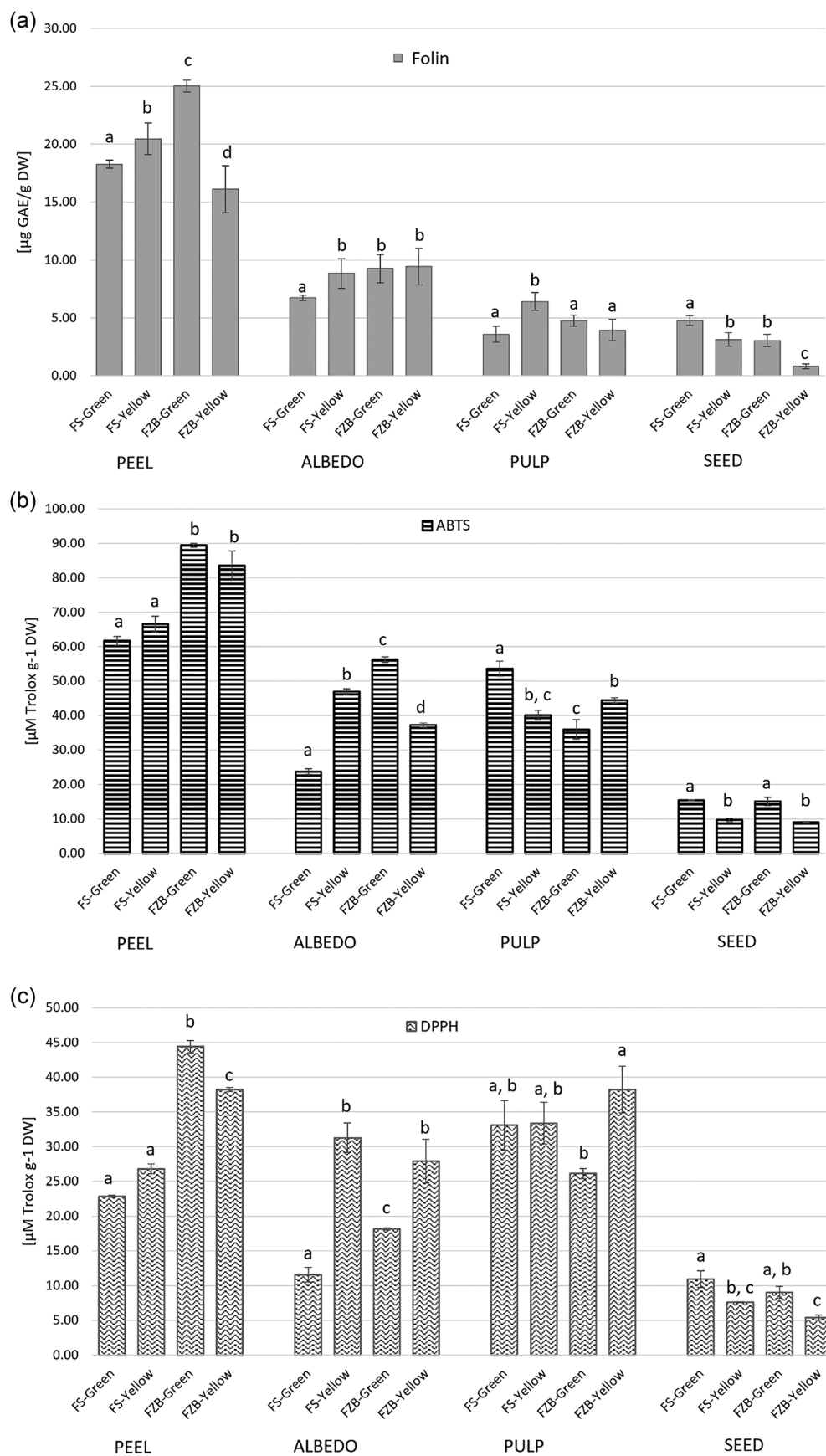


FIGURE 1 Comparison of phenolic compounds and antioxidant activity measured through Folin–Ciocalteu (a), ABTS (b), and DPPH (c) assays among the analyzed samples. Values are expressed as mean \pm standard deviation (SD) of three independent experiments. Letters indicate significant differences between experiments ($p < 0.05$).

and 2,2-azinobis-(3-ethylbenzothiazoline-6-sulfonate radical cation) (ABTS^{•+}) by the slightly modified methods previously described (Cannavacciuolo et al., 2023). Briefly, an aliquot (50 µL) of the extract (1 mg mL⁻¹) or standard solution (2.5–10 µg mL⁻¹) was added to 950 µL of prepared DPPH[•] radical solution (0.14 mM). After darkness incubation for 30 min at room temperature, samples were read by spectrophotometer at a wavelength of 515 nm. For the ABTS^{•+} scavenging activity, the reaction was initiated by the addition of 50 µL of extract in 950 µL of diluted ABTS (14 mM) of each sample solution. The spectrophotometer was set with a wavelength of 734 nm. Determinations were repeated three times. The absorbance was calculated for each concentration relative to a blank absorbance (methanol) and plotted as a function of the concentration of compound or standard, 6-hydroxy-2,5,7,8-tetramethylchroman-2-carboxylic acid (Trolox). The antioxidant activity was expressed as Trolox equivalents (TE) value representing the µmol of a standard Trolox solution in 1 g of dry matrix (DW) and reported in Figure 1B,C.

2.6 | UHPLC–QTOF–HRMS/MS profile of citrus extracts

UHPLC–QTOF–HRMS/MS analyses were performed using an electrospray ionization (ESI) source coupled with liquid chromatography and HRMS system, a Waters ACQUITY UPLC system coupled with a Waters Xevo G2-XS QToF mass spectrometer (Waters Corp.), operating in negative and positive ionization modes. Chromatographic separation was performed using a Biphenyl column (100 mm × 2.1 mm, 2.6 µm; Phenomenex) and the mobile phase consisting of 0.1% (v/v) formic acid in water (A) and 0.1% (v/v) formic acid in acetonitrile (B) at a flow rate of 0.4 mL min⁻¹. A linear gradient from 5% to 10% B was held for 2 min; up to 80% B from 2.0 to 17.0 min; and up to 95% B for 1 min. A column wash at 95% B was held for 5 min and a column equilibration for 3 min (5% B) before the next injection subsequent analysis. The autosampler was set to inject 5 µL of each sample at a concentration of 0.5 mg mL⁻¹. For the ESI source, the following experimental conditions were adopted: electrospray capillary voltage of 2.5 kV, source temperature of 150°C, and desolvation temperature of 500°C. MS spectra were acquired by full-range acquisition, covering a mass range of 50–1200 *m/z*. HRMS/MS analysis was performed by data-dependent scanning experiments, selecting the first and second most intense ions from the HRMS scan event and subjecting them to collision-induced dissociation by applying the following conditions: the minimum signal threshold at 250, isolation width at 2.0, and normalized

collision energy at 30%. In both full scan and MS/MS modes, a resolving power of 30,000 was used. Chemical deconvolution was attributed using UNIFI software, matching MS/MS spectra with Chemspider database along with a self-made library of phenolic compounds and confirmation with literature reports.

2.7 | Semiquantitative analysis by UHPLC–UV

For quantitative analysis, stock solutions (1 mg mL⁻¹) of the compounds used as external standards were prepared by dissolving each compound in a methanol/water solution (50% v/v). Increasing solution concentrations (0.1, 0.5, 1, 5, 10, and 50 µg mL⁻¹) were prepared for calibration curve construction by UHPLC–UV analysis, with wavelength set at 280 nm. Specifically, 5 µL of each standard solution of each concentration was injected into a technical triplicate. Calibration curves were obtained by linear regression using Excel 2016 software, considering the area of the external standards versus the known concentration of each compound. The obtained calibration curves showed good linearity with correlation coefficients (*R*²) ranging from 0.9969 to 0.9999. Quantitative data are expressed as mg g⁻¹ dry extract (EXT). MassLynx software (version 4.2) was used for instrument control, data acquisition, and processing.

2.8 | Multivariate statistical analysis

A complex dataset containing UHPLC–HRMS data of all investigated compounds was organized, containing 27 variables (metabolites tentatively identified) and 16 observations as follows: x2 ripening stages (green and yellow), x4 parts (peels, pulp, albedo, and seeds), x2 cultivar (FS and FZB). To observe the comprehensive distribution of the metabolites in all four samples, the integrations (AUC) of UHPLC–HRMS signals were selected in the matrices and normalized by average function. The obtained dataset was processed by SIMCA[®]18 (Sartorius) for statistical analysis and modeling of score and loading plots. PCA and PLS models were described by two main principal components, scaled by Pareto mode and Autofit functions. For reproducibility of the analysis, three extraction replicates and three replicate injections per sample extract were provided in a random way. Periodical injections of extraction solvent (blank) and a sample mix containing all the samples (QC) were analyzed for each five-acquisition batch. The results of QC were centered on ensuring the reproducibility, the stability of the MS signals during the full acquisition batch, and the robustness of the chemometric results.

2.9 | Statistical analysis

UHPLC–HRMS experiments were performed in technical triplicate and biological duplicate. DPPH and ABTS radical scavenging tests were performed in triplicate, and the results were expressed as mean \pm SD. The values were compared using the Tukey test following a one-way analysis of variance calculation using JMP statistical discovery software (version 17). A p -value <0.05 was considered to be statistically significant. The PCA and PLS were considered imaging techniques, operating the linear regressions on the mean-scaled dataset to select the two main principal components in a multivariate data analysis approach (RIF). The choice of principal components was established based on the fitting (R^2X , 0.719) and predictive (Q^2X , 0.484) values. For PCA models, the chosen first principal component (PC1) and second principal component (PC2) explained 56.4% and 15.5% of the variance, respectively, for a total explained variance of 71.9%. The PLS analysis showed a distinct separation (R^2X , 0.717; R^2Y , 0.872) and good predictability (Q^2 , 0.741). No outliers were detected at a confidence level of 95% based on Hotelling's T^2 and Q residual statistical tests.

2.10 | Zebrafish maintenance

Zebrafish ABO (*D. rerio*) were bred at the European Zebrafish Resource Center-EZRC (Karlsruhe Institute of Technology, Karlsruhe, Germany) in a flow-through system (Aqua Schwarz and Müller + Pfleger). Adult zebrafish were raised in 15-L tanks containing a maximum of 24 individuals and under a 14-h:10-h light–dark cycle. The water had a temperature of 28.5°C and a conductivity of 200 μ S and was continuously renewed. The fish were fed three times a day, with dry food and *Artemia salina* larvae. The afternoon before spawning, several groups of females and males (1:1) were introduced into 1 L breeding tanks (Tecniplast S.p.A.). Immediately after spawning, fertilized eggs were collected with a sieve. Eggs were transferred to Petri dishes with Embryos Medium (E3), and non-fertilized eggs or embryos with injuries were discarded.

2.11 | Fish embryo toxicity test assessment of acute toxicity and LC50

Fish embryo acute toxicity tests (fish embryo toxicity [FET] tests), a robust method to assess the acute toxicity, were performed according to OECD n. 236 (OECD, 2013). “Feminello Zagara Bianca” green peel was dissolved in E3 medium, reaching the final concentration of 12.5, 25, 50, 100, 200, 400, and 800 μ g mL⁻¹.

Selected embryos were placed individually with 2 mL of solution in each well of 24-well plates. For each experimental plate, 4 wells with E3 medium were employed as internal plate control, and 20 embryos per concentration were exposed to the natural extract; the working solutions were renewed every 24 h. Moreover, one negative control plate (E3 medium) and one positive control plate (4% 3,4-dichloroaniline) were also tested. Embryos were incubated for 96 hpf at 28.5°C. Embryos were daily observed up to 96 h with the stereomicroscope (Nikon SMZ645), recording the following four apical observations as indicators of lethality: coagulation of fertilized eggs, lack of somite formation, lack of detachment of the tail-bud from the yolk sac, and absence of heartbeat. During the exposure period, the percentage of the hatching rate was also recorded from 48 hpf, every 24 h. Experiments were repeated three times in different weeks.

2.12 | Data analysis fish embryo toxicity (FET) test

The concentration–response curves from the FET data were analyzed using the PROAST web-tool for BMD analysis, based on the PROAST software version 70.1 developed by the Dutch Institute for Public Health and the Environment (RIVM, The Netherlands) (Slob, 2002), in which the benchmark concentration (BMC) at a predefined benchmark response (BMR) was calculated using a fitted dose–response curve. The LC50 was determined from the concentration–response curves obtained in the FET using the same PROAST web-tool for BMD analysis. To this purpose, the BMR was set to 50%, representing the concentration causing either 50% cumulative mortality or lethality (LC50).

Figures of concentration–response curves for the effect of test compounds in the FET were made using GraphPad Prism 8.0.

3 | RESULTS AND DISCUSSION

3.1 | Preliminary antioxidant evaluations

In order to select the extract with higher radical-scavenging activity correlated with the content of bioactive compounds, preliminary spectrophotometric assays were performed. All the obtained extracts were tested by Folin–Ciocalteu, ABTS, and DPPH assays, followed by UHPLC–HRMS analysis for a deep chemical characterization. The comparison of the TPC, DPPH, and ABTS data reported in Figure 1 suggested that the peels showed higher antioxidant capacity than pulp, albedo, and seeds, which

did not show considerable variability. Based on previous results, the differences between green or yellow ripening stages of both FS and FZB were considered. In particular, green peels showed TPC, with values of 18.27 ± 1.35 and $25.03 \pm 1.50 \mu\text{g GAE g}^{-1}$ DW for FS and FZB, respectively, compared to yellow peels values of 20.47 ± 1.37 and $16.11 \pm 2.03 \mu\text{g GAE g}^{-1}$ DW for FS and FZB, respectively, with statistical differences only between FS and FZB cultivars and not between ripening stages (Figure 1A). The general overview of preliminary antioxidant assays reveals that the peels of FZB at the green stage provided the most representative content of phenols; $25.03 \pm 1.50 \mu\text{g GAE/g DW}$ is also characterized by the highest preliminary activity in quenching ABTS and DPPH radicals, 89.42 ± 2.53 and $44.40 \pm 1.88 \mu\text{M Trolox g}^{-1}$ DW, respectively (Figure 1B,C). These results are in agreement with the study on *Citrus x limon* peels conducted by Mcharek, who reported 23.07 and $82.01 \mu\text{M Trolox g}^{-1}$ DW values for DPPH and ABTS, respectively (Mcharek & Hanchi, 2017). In addition, comparing these two cultivars with other species of the *Citrus* genus, it can be seen that their antioxidant potency is similar to that found in wild mandarin peel, with antioxidant activity ranging between 65.62–108.06 and 25.14–50.46 $\mu\text{M Trolox g}^{-1}$ DM in the ABTS and DPPH assays, respectively (Zhang et al., 2014), but higher than the antioxidant capacity of kaffir lime peel ($12.02 \pm 1.02 \mu\text{M Trolox g}^{-1}$ DW in DPPH assay) (Lubinska-Szczygeł et al., 2023).

3.2 | Chemical characterization by using UHPLC–HRMS/MS analysis

The obtained citrus extracts were analyzed by UHPLC–DAD–(–/+)-HRMS/MS to investigate their qualitative profiles. Figure S1 shows a representative UHPLC chromatogram at 280 nm of FZB in green stage extract. A total of 36 peaks were tentatively identified. Metabolite assignments were made by comparing retention time, UV/Vis spectra, and MS data (accurate mass and MS fragment of the compounds detected with standard compounds, whenever available, and compounds reported in the literature and databases). The identities, retention times, and MS data of each compound are listed in Table 2.

3.2.1 | Identification of flavonoids

Flavonoids are a heterogeneous group of polyphenols characterized by high antioxidant activity, widely distributed in *Citrus*. Their different occurrences among the different species and varieties affect the appearance, taste, and nutritional value of the fruit. Generally, flavonoids in

plants could be in both aglycone or glycosylated form with sugar moieties of hexoses, deoxyhexoses, or pentoses. Depending on the linkage of sugar moieties to the flavonoid aglycone, C- and O-glycosides are easily distinguishable by unambiguous MS/MS spectra, depending on the nature of the sugar unit. In particular, compounds 6–8, 11, 18, 21, and 22 (Table 1) belong to C-glycosides generating MS/MS neutral losses of 30, 90, and 120 Da in the case of hexose sugars, 74 and 104 Da in the case of deoxyhexose sugars, and 60 Da for pentose sugars (Table 1). Compounds 13–16, 20, 23, 25, 26, and 30 (Table 1) are characterized by an O-glycosylation pattern in MS/MS spectra due to the neutral loss of 162 Da (hexose sugar), 146 Da (deoxyhexose sugar), and 132 Da (pentose sugar). Compounds 17, 28, 31, 33–36 are aglycone scaffold flavonoids occurring in the final part of UHPLC–HRMS chromatogram (Table 1). Compounds 6 and 13 showed a similar $[\text{M}-\text{H}]^-$ parent ion at m/z 609.1463 and m/z 609.1458, respectively, with a molecular formula $\text{C}_{27}\text{H}_{30}\text{O}_{16}$. The retention times and MS/MS spectra reveal their different chemical behaviors. In fact, the detailed analysis of HRMS/MS spectra assigned compound 6 to lucenin 2 and compound 13 to rutin due to the characteristic fragmentation patterns. In particular, the MS/MS spectra of compound 6 show m/z at 519.1145 and m/z at 489.1039, related to the loss of the first C-glycoside residue along with the presence of m/z at 399.0719 and 369.0612, attributed to the loss of the second C-glycoside residue. The match with MS/MS spectrum is related to lucenin 2 (Cannavacciuolo et al., 2023). The product ion 300.1458 $[\text{M}-(\text{C}_{12}\text{H}_{22}\text{O}_{11})-\text{H}]^-$ in the MS/MS spectrum of compound 13 corresponds to the neutral loss of a rutinoside unit formed by a deoxyhexose sugar (146 Da) and hexose moiety (162 Da) linked via O-glycosylation to the scaffold. The resulting aglycone with m/z 300.0267 was identified as quercetin due to the formation of a characteristic fragment of m/z 271.0241 (Śliwka-Kaszyńska et al., 2022). Flavonoids are powerful antioxidants that scavenge free radicals due to the presence of the hydroxyl group in their structure and their ability to donate hydrogen and chelate metal ions (Parcheta et al., 2021; Tripoli et al., 2007). In addition, studies have shown that flavonoids can suppress enzymes involved in ROS production. They are also known for their ability to prevent lipid peroxidation caused by oxidative stress (Galleano et al., 2010; Procházková et al., 2011). Finally, certain flavonoids, such as hesperidin, apigenin, and luteolin, can influence the function of enzyme systems involved in inflammatory processes, for example, by inhibiting nitric oxide isoform synthase, cyclooxygenase, and lipoxygenase, enzymes involved in the production of inflammatory mediators, thus having potential anti-inflammatory activity (Kumar & Pandey, 2013).

TABLE 1 List of compounds putatively identified by ultrahigh-performance liquid chromatography (UHPLC)-QTOF-high-resolution mass spectrometry (HRMS)/MS analysis.

n	Rt (min)	[M-H] ⁻	[M+H] ⁺	Compound	Molecular formula	Δppm	MS/MS	IL	Reference
1	0.59	191.0554		Quinic acid	C ₇ H ₁₂ O ₆	-3.8	173.0441/127.0389/ 71.0130	2	Chempider
2	3.42	355.0669		<i>p</i> -Coumaroyl aldaric acid isomer 1	C ₁₅ H ₁₆ O ₁₀	-0.4	265.0346/191.0190/ 173.0080/163.0391/ 147.0287/119.0492	2	Dueñas et al. (2015)
3	4.95	355.0669		<i>p</i> -Coumaroyl aldaric acid isomer 2	C ₁₅ H ₁₆ O ₁₀	-0.9	209.0293/191.0190/ 173.0080/163.0391/ 147.0287/119.0492	2	Dueñas et al. (2015)
4	5.05	355.0669		<i>p</i> -Coumaroyl aldaric acid isomer 3	C ₁₅ H ₁₆ O ₁₀	-0.7	209.0293/191.0190/ 173.0080/163.0391/ 147.0287/119.0492	2	Dueñas et al. (2015)
5	6.28	365.1450		Propyl-HMG-hexoside	C ₁₅ H ₂₆ O ₁₀	-0.9	221.1020/161.0446/ 125.0235/101.0234	3	Zhang et al. (2022)
6	7.99	609.1463		Lucenin 2	C ₂₇ H ₃₀ O ₁₆	0.3	519.1145/489.1039/ 399.0719/369.0612/ 177.0184	2	Otiŷy et al. (2015)
7	8.99	593.1519		Apigenin 6,8-di- <i>C</i> -hexoside	C ₂₇ H ₃₀ O ₁₅	1.2	503.1090/473.0950/ 383.0639/353.0512	2	Otiŷy et al. (2015)
8	9.55	447.0925		Orientin	C ₂₁ H ₂₀ O ₁₁	-1.7	357.0603/327.0499/ 297.0393/133.0285	2	Pereira et al. (2012)
9	9.72		193.0493	Isoscopoletin	C ₁₀ H ₈ O ₄	-1.4	178.0255/150.0306/ 133.0279/122.0355	2	Chempider
10	10.30		565.1552	Lucidin primeveroside	C ₂₆ H ₂₈ O ₁₄	0	433.1126/415.1018/ 313.0700/283.0595/ 271.0594	2	Chempider
11	10.39	623.1616		Chrysoeriol 6,8-di- <i>C</i> -glucoside	C ₂₈ H ₃₂ O ₁₆	-0.3	503.1044/413.0718/ 383.0598/191.0335	2	Gattuso et al. (2006)
12	10.66		163.0386	3-Hydroxycoumarin	C ₉ H ₆ O ₃	-2.5	107.0487	2	Chempider
13	10.68	609.1458		Rutin	C ₂₇ H ₃₀ O ₁₆	1.9	300.0267/271.0241	1	Std
14	10.84	431.0978		Apigenin-7- <i>O</i> -glucoside	C ₂₁ H ₂₀ O ₁₀	1.2	341.0656/311.0551/ 283.0601/269.0442	2	March et al. (2006)
15	11.08	595.1688	597.1811	Eriocitrin	C ₂₇ H ₃₂ O ₁₅	3.3	287.0552/151.0029	1	Std
16	11.10	435.1281		Naringenin-7- <i>O</i> -glucoside	C ₂₁ H ₂₂ O ₁₀	-1.0	381.0698/289.0698/ 263.0543/245.0436/ 219.0280/195.0281/ 165.0175/153.0175	2	Gao et al. (2022)
17	11.17		287.0547	Kaempferol	C ₁₅ H ₁₀ O ₆	-1.1	163.0382/153.0178	2	Chempider

(Continues)

TABLE 1 (Continued)

n	Rt (min)	[M-H] ⁻	[M+H] ⁺	Compound	Molecular formula	Δppm	MS/MS	IL	Reference
18	11.22	607.1667		Zivulgarin	C ₂₈ H ₃₂ O ₁₅	-0.3	443.0970/323.0552/ 101.0242	2	Chempider
19	11.35		193.0492	Scopoletin	C ₁₀ H ₈ O ₄	-1.9	178.0255/150.0306/ 133.0279/122.0355	2	Yang et al. (2010) and Zhang et al. (2022)
20	11.87	623.1622		Isorhamnetin-3-O- rutinoside	C ₂₈ H ₃₂ O ₁₆	0.8	315.0497/300.0260/ 151.0026	2	El-Zahar et al. (2022)
21	12.09	461.1082		Scoparin	C ₂₂ H ₂₂ O ₁₁	-1.7	371.0761/341.0657/ 298.0472	2	Gattuso et al. (2006)
22	12.15		463.1235	Diosmetin-C-glucoside	C ₂₂ H ₂₂ O ₁₁	0.1	379.0810/367.0807/ 343.0810/313.0703/ 298.0467	2	Fu et al. (2016)
23	12.28	579.1704		Naringenin-7-O- rutinoside	C ₂₇ H ₃₂ O ₁₄	-2.6	459.1144/271.0606/ 151.0029	2	Mullen et al. (2008)
24	12.41		147.0439	Coumarin	C ₉ H ₆ O ₂	-1.3	119.0482/101.0385	2	Chempider
25	12.60	607.1671		Diosmin	C ₂₈ H ₃₂ O ₁₅	0.4	299.0553/284.0317/ 161.0231	2	Zhang et al. (2022)
26	12.78	609.1824		Hesperidin	C ₂₈ H ₃₄ O ₁₅	-0.1	301.0711	2	Mullen et al. (2008)
27	12.87	651.1567		Tetrahydroxydimethoxy flavone HMG-hexoside	C ₂₉ H ₃₂ O ₁₇	0.5	607.1673; 589.1590 549.1228; 507.1143 345.0618	3	Fu et al. (2016)
28	12.95	287.0561		Eriocytrol	C ₁₅ H ₁₂ O ₆	-0.2	151.0029/135.0444	2	Santos et al. (2010)
29	13.04	681.1729		Limocitrol-HMG-O- hexoside	C ₃₀ H ₃₄ O ₁₈	1.2	619.1671/579.1359/ 537.1250/375.0719/ 360.0487	2	El-Sayed et al. (2017)
30	13.27	609.1817	611.1817	Chrysoeriol 7-O-rutinoside	C ₂₈ H ₃₂ O ₁₅	0.4	301.0702/286.0465	2	Min Vivian Goh et al. (2022)
31	13.50		287.0549	Luteolin	C ₁₅ H ₁₀ O ₆	-0.6	153.0178	1	Std
32	13.70	765.1889		Isorhamnetin-di-HMG- O-glycoside	C ₃₄ H ₃₈ O ₂₀	0.7	503.1196/473.1090/ 383.0770/353.0663	2	Cannavacciuolo et al. (2023)
33	15.09	299.0556	301.0703	Diosmetin	C ₁₆ H ₁₂ O ₆	-1.7	284.0319/256.0368	2	Hamdan et al. (2020)
34	15.19	345.0612		Limocitrin	C ₁₇ H ₁₄ O ₈	-1.3	330.0371/315.0136	2	Chempider
35	15.37	301.0716		Hesperitin	C ₁₆ H ₁₄ O ₆	-0.7	285.0394/164.0105/ 136.0157/1088.0204	1	Std
36	15.50	375.0730		Limocitrol	C ₁₈ H ₁₆ O ₉	2.3	360.0481/317.0298/ 302.0062/274.0111	2	El-Sayed et al. (2017)

Abbreviation: IL, identification level according to Metabolomics Standards Initiative.

3.2.2 | Identification of HMG-flavonoids

Compounds 27, 29, and 32 (Table 1) showed typical HRMS/MS signals of 3-hydroxy-3-methylglutaryl (HMG) moiety linked to phenolic residues as the loss of 144 Da ($C_6H_8O_4$) (Table 1). The MS/MS spectrum of compound 29 (m/z 681.1729) showed an ion $[M-144-H]^-$ at m/z 537.1250 along with the fragment $[M-162-144-H]^-$ at m/z 375.0719, suggesting the presence of HMG moiety and the glycosyl group attached to the aglycone as the identities of limocitrol-HMG-O-hexoside (El-Sayed et al., 2017).

3.2.3 | Identification of coumarins

The extracts showed the occurrence of coumarins investigated with a good MS response in positive mode (Table 1). Generally, coumarins exhibited a distinct fragment ion, $[M-CO_2+H]^+$ from the pyran-2-one scaffold. The described fragmentation pattern could be diagnostic for the characterization of coumarins in the fruit, as in the case of the peaks 9, 12, 19, and 24 (Table 1). In particular, compound 19 showed a molecular formula of $C_{10}H_8O_4$ calculated for $[M+H]^+$ ion at m/z 193.0492. The $[M-CO_2+H]^+$ ion at m/z 150.0306 allowed the identification of scopoletin (Yang et al., 2010; Zhang et al., 2022). Coumarins are known for their health benefits, such as lowering the risk of chronic diseases, such as cancer (Garg et al., 2020), cardiovascular diseases (Najmanová et al., 2015), and neurodegenerative disorders, managing inflammatory conditions such as arthritis (Miao et al., 2021), and preventing neurodegenerative diseases like Alzheimer's (Liu et al., 2022-b), and Parkinson's disease (Wang et al., 2024).

3.3 | Principal component analysis

The different ripening stages (green and yellow, respectively), along with the parts of the lemon fruit (peels, pulp, albedo, and seeds) of both FS and FZB cultivars, were considered main variables in the modeled sample discrimination. The distribution of the samples was performed by PCA, the score plot of which shows that the PC1 divided the peels of FS and FZB in both green and yellow growth stages, on the right part of the PCA score plot ($PC1 > 0$) highlighted in red cluster (Figure 2A). The incidence of the metabolites on the following clusterization is related to their distance from the origin in the loading plot (Figure 1B). In particular, compounds 1, 4 (quinic acid and p-coumaroyl aldaric acid isomers, respectively), along with the C-glycoside flavonoids (compounds 6 and 7) and

HMG-flavonoids (compounds 29 and 32), and the aglycone (compound 34), positively affected the cluster discrimination with higher incidence (Figure 2B). The blue cluster on the upper left quadrant of the score plot ($PC1 > 0$; $PC2 < 0$) contained albedo samples of both FS and FZB in both green and yellow stages (Figure 2A). This cluster is discriminated for the occurrence of compounds 3, 14, and 23, mainly affecting the distance from the origin of the loading plot (Figure 2B). The samples of seeds and pulp were plotted without significant separation in the bottom left quadrant with $PC1 < 0$ and $PC2 < 0$ as shown by the green cluster in PCA score plot (Figure 2A).

3.4 | Partial least squares analysis

The correlation between the large set of samples and preliminary antioxidant activity was provided by PLS analysis with the aim of selecting the extract with more interesting activity for further in vivo investigation (D'Urso et al., 2018; Garcia et al., 2023; Pagliari et al., 2022). In particular, PLS was performed for the attribution of metabolites to the hydroalcoholic extracts based on the different capacities to quench DPPH and ABTS radicals among the samples (RIF) of peel, pulp, and albedo in both green and yellow growing stages. The PC1 of PLS score plot (Figure 3A) separates the peel ($PC1 > 0$) on the right part of the plot against pulp, seeds, and albedo on the left part of the plot ($PC1 < 0$), whereas the PC2 separates the FZB cultivar ($PC2 < 0$) from FS cultivar ($PC2 > 0$) (Figure 3A). The loading plot shows metabolites that significantly affected the discrimination of samples observed in the score scatter plot (Figure 3B). The incidence of compounds 1, 4, 6, 7, 29, and 34 (Table 1) determined the distribution of the peels, which was characterized by the higher activity in both DPPH and ABTS assays. Among the peels of investigated lemon fruits, the FZB in the early stage of growth (green) was the most positively affected by the PLS discrimination, far away from the origin of the score plot (Figure 3A).

3.5 | Semiquantitative analysis

The descriptive metabolomic workflow drove the selection of the extract with higher activity related to compounds that occurred for further in vivo investigations. For in vivo evaluation of dose-dependent toxicity, a semiquantitative analysis of major phenolic compounds and coumarins occurring in the selected extract was performed. The quantification was carried out by UHPLC-UV analyses at a wavelength of 280 nm using calibration curves of available standards in a range of $0.1-50 \mu g mL^{-1}$ (Table 2). Compounds for which reference standards were not

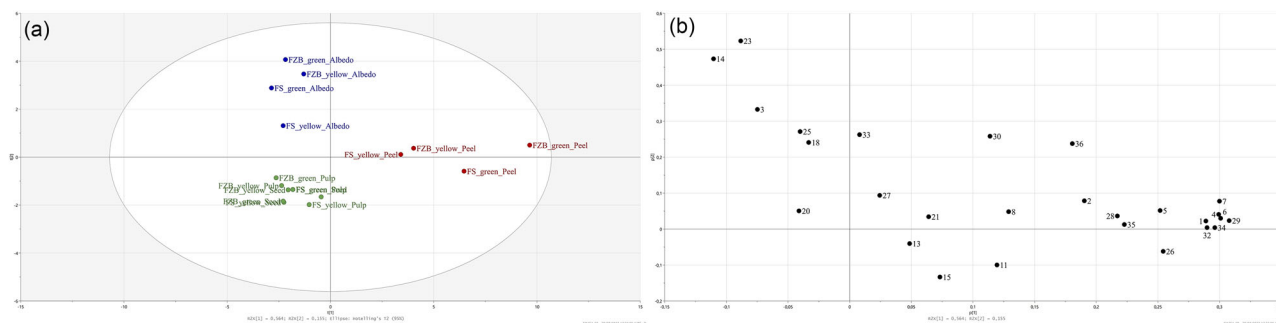


FIGURE 2 Principal component analysis (PCA) score plot (a) and loading plot (b) performed on the peels (red cluster), albedo (blue cluster), pulp, and seeds (green cluster).

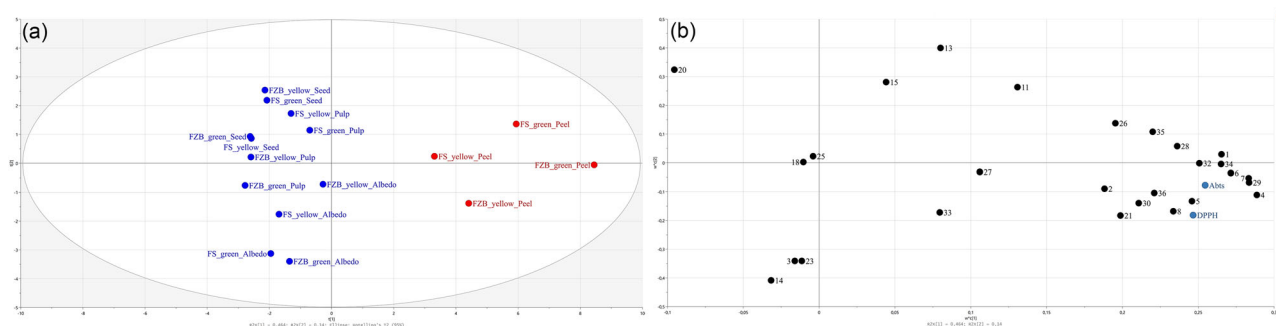


FIGURE 3 Partial least squares (PLS) score plot (a) and loading plot (b) performed on the peels (red cluster), albedo, pulp, and seeds (blue cluster).

available were quantified into standard equivalents using the most chemically related standard available. The higher phenolic compounds occurring in the peel extract were the C-glycoside orientin (compound 8) at $1104.39 \pm 46.76 \mu\text{g g}^{-1}$ EXT, followed by the O-glycoside eriocitrin (compound 15) at $1041.17 \pm 29.64 \mu\text{g g}^{-1}$ EXT. Lemon and citrus fruits containing eriocitrin and orientin as major polyphenolic components are recognized for their anti-inflammatory, nephroprotective, neuroprotective, cardioprotective, and other pharmacological benefits (Jing et al., 2020; Lam et al., 2016; Wan et al., 2020; Yao et al., 2022). Among coumarins, compound 24 (coumarin) showed the higher amount at $339.69 \pm 16.22 \mu\text{g g}^{-1}$ EXT.

3.6 | The LC50 value of FZB green peel on zebrafish embryos

FET test acceptance criteria were achieved by following OECD n. 236 as the mortality of negative control at 96 hpf was 0% and the mortality in the positive control group was 35% (Figures 4 and 5). In the positive control group, embryos treated with 4% of 3,4-dichloroaniline developed severe yolk sac and cardiac edema (Figure 5). This inflammatory phenotype is caused by the significant increase

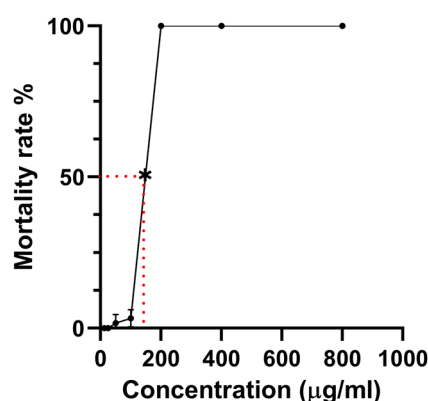


FIGURE 4 Fish embryo toxicity (FET) test. Effect of seven concentrations (12.5, 25, 50, 100, 200, 400, and 800 $\mu\text{g mL}^{-1}$) of Femminello Zagara Bianca (FZB) green peel on zebrafish embryo mortality. The LC50 value was $107.833 \mu\text{g mL}^{-1}$. Values are expressed as a mean \pm standard deviation (SD) of three independent experiments.

in ROS production resulting from DCA treatment (Hasoun et al., 2005). Moreover, DCA treatment had effects on mobility, as evidenced by an altered escape response to touch. The FZB green peel treatment mortality rate of the zebrafish at 96 hpf was 100% for all concentrations

TABLE 2 Quantitative analysis of main compounds in lemon extracts.

N	Compounds	std	$\mu\text{g g}^{-1}$ EXT
6	Lucenin 2	Luteolin	1012.07 ± 58.25
7	Apigenin 6,8-di-C-hexoside	Apigenin	608.96 ± 22.16
8	Orientin	Luteolin	1104.39 ± 46.76
9	Isoscapoletin	Cumarin	294.82 ± 35.36
12	3-Hydroxycoumarin	Cumarin	333.44 ± 31.50
13	Rutin	Rutin	547.65 ± 12.87
14	Apigenin-7-O-glucoside	Apigenin	495.73 ± 32.01
15	Eriocitrin	Eriocitrin	1041.17 ± 29.64
16	Naringenin-7-glucoside	Naringenin	303.04 ± 22.28
19	Scopoletin	Coumarin	286.61 ± 17.67
23	Naringenin-7-O-rutinoside	Naringenin	329.44 ± 21.25
24	Coumarin	Coumarin	339.69 ± 16.22
26	Hesperidin	Hesperitin	493.01 ± 20.05
28	Eriocytrol	Eriocitrin	700.20 ± 48.91
31	Luteolin	Luteolin	971.16 ± 55.31
35	Hesperitin	Hesperitin	517.80 ± 33.08

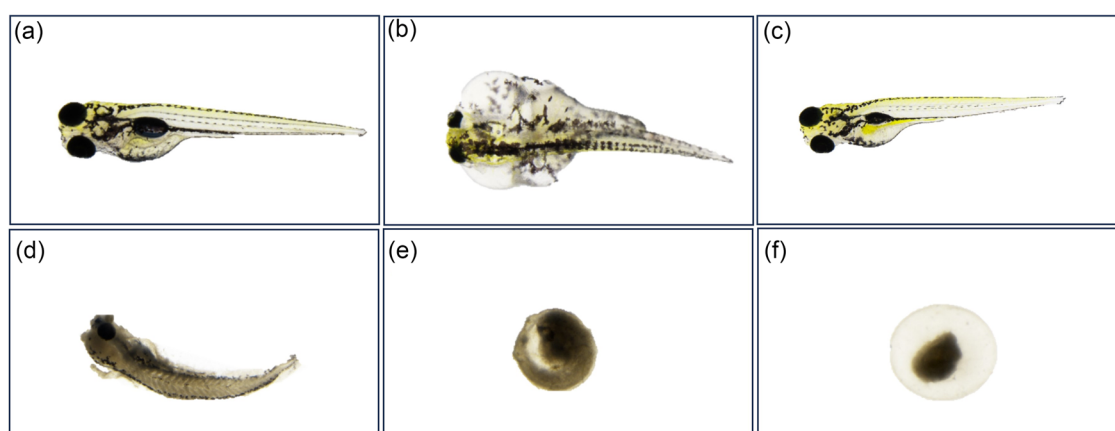


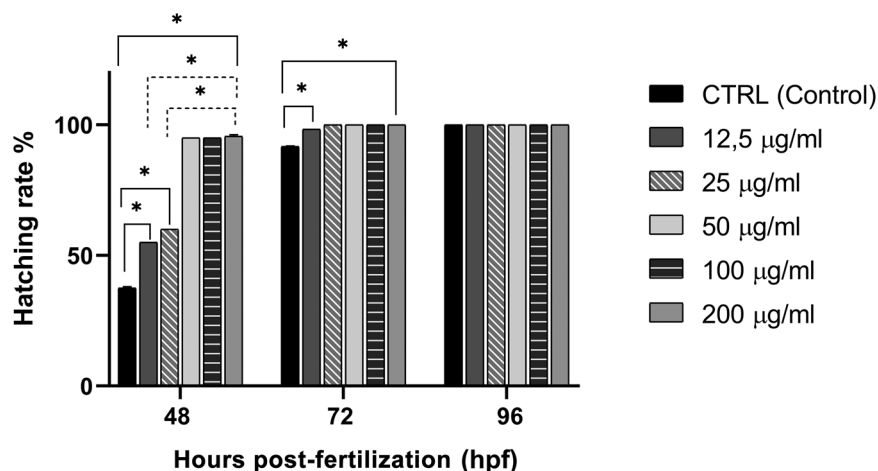
FIGURE 5 Toxicity of Femminello Zagara Bianca (FZB) green peel in zebrafish embryo 96 hpf testing: (a) normal phenotype of the negative control (E3 medium), (b) abnormal phenotype of the 3,4-dichloroaniline ($4 \mu\text{g mL}^{-1}$) positive control embryo, (c) normal phenotype of the *Citrus limon* [$12.5\text{--}100 \mu\text{g mL}^{-1}$] treated embryo, (d–f) representative phenotypes of dead embryo treated with 200, 400, and $800 \mu\text{g mL}^{-1}$ of FZB green peel.

ranging from 200 up to $800 \mu\text{g mL}^{-1}$. Figure 5 shows the different treatment-induced larval phenotypes. At 48 hpf, 100% mortality was observed at the highest concentration of $800 \mu\text{g mL}^{-1}$ and 50% mortality at $400 \mu\text{g mL}^{-1}$, showing stronger acute toxicity than at lower concentrations. The FZB green peel treatment was observed to demonstrate 5% of mortality rate at 96 hpf at the intermediate concentrations of 100 and $50 \mu\text{g mL}^{-1}$, whereas at the lower concentrations of 25 and $12.5 \mu\text{g mL}^{-1}$, the FZB green peel showed no lethal effects. The resulting LC50 value at 96 hpf was $107,833 \mu\text{g mL}^{-1}$, whereas BMD confidence intervals were $102\text{--}195 \mu\text{g mL}^{-1}$.

3.7 | The Effects of FZB green peel on the embryo hatching rate

Hatching of zebrafish embryos, under standard housing conditions, occurs between 48 and 72 h post-fertilization, whereas data recorded during FET observations indicate different hatching rate trends in the extract-treated groups, as shown in Figure 6. At 48 hpf, 55% and 60% of the embryos were hatched, respectively, at the lower concentrations of 12.5 and $25 \mu\text{g mL}^{-1}$; overall, 95% hatching rate was observed at the higher concentrations (50, 100, and $200 \mu\text{g mL}^{-1}$), whereas only 37.5% of the embryos were

FIGURE 6 Effect of different concentrations of Femminello Zagara Bianca (FZB) green peel on hatching rate. Values are expressed as the mean \pm standard deviation (SD) of three independent experiments. Asterisks indicate significant differences between treatment and control groups (Student *t*-test, $p < 0.05$).



hatched in the control group (E3 medium). No hatching was observed at the higher concentrations of 800 and 400 $\mu\text{g mL}^{-1}$ as a result of embryo mortality. At 72 hpf, all the groups treated with FZB green peel were out of the chorion, except at the lowest concentration (12.5 $\mu\text{g mL}^{-1}$) that reached 98% of hatching, which was higher when compared with the control group (E3 medium) that in the same interval reached 91.7%. At the end of the FET trial, the above two groups also achieved 100% hatching. Compared to the control group, the hatching rate of zebrafish embryos exposed to various doses of FZB green peel exhibited a statistically significant acceleration in a treatment- and dose-dependent manner ($p < 0.05$). The increased hatching rate timings in the treated groups with *Citrus maxima* peel extract are also reported in the literature (Dananjaya et al., 2020).

4 | CONCLUSION

This study demonstrated that *Citrus x limon* peels obtained as agri-food industrial waste are a potential source of raw materials for the extraction of natural products with potential health benefits. In particular, the industrial byproducts (peel, pulp, albedo, and seeds) of two specific cultivars, commonly called “Femminello Siracusano” (FS) and “Femminello Zagara Bianca” (FZB), grown in southern Italy (Sicily region), were analyzed and compared for their chemical compounds. The development of a UHPLC–ESI–HRMS/MS method, in positive and negative ionization mode, allowed the detection and characterization of 36 secondary metabolites belonging to the flavonoid, HMG-flavonoid, and coumarin groups, confirming lemon as an excellent source of phenolic substances. The antioxidant power of each sample was tested using spectrophotometric assays (DPPH and ABTS), and the peel samples were found to be the byproduct with the highest antioxidant power. In addition, multivariate PCA and PLS analyses were used to

compare the metabolic profile with the antioxidant activity tested in vitro. The results identified metabolites 1, 4, 6, 7, 29, and 34 as the most influential in the selection of peels, particularly that of the green FZB stage, which was confirmed to be the richest in bioactive polyphenols. These findings highlight the possible use of lemon peel extract to reduce oxidative stress, lower the risk of chronic diseases such as cancer, cardiovascular diseases, and neurodegenerative disorders, and manage inflammatory conditions. Finally, flavonoids and coumarins were identified and quantified in the extract for the evaluation of in vivo toxicity through the FET, a necessary step to determine the safe dose to be used in the subsequent experimentation stages. The FZB green peel extract significantly accelerated the hatching rate, suggesting that it could mimic the luteinizing hormone-releasing hormone, allowing better control of breeding cycles. In summary, the use of zebrafish embryo toxicity testing holds promise as an initial screening approach and potentially as a substitute for mammalian toxicity testing. As countries strive to minimize mammalian animal testing, the zebrafish embryo is gaining recognition as a feasible alternative for prioritizing compounds in developmental toxicity testing among higher vertebrates. Furthermore, the results of this study provide a better understanding of *Citrus x limon* primary chemical bioactives and in vivo safety, particularly for the cultivar “Femminello Zagara Bianca” at the early ripening stage. In line with reported data, the peel of the “Femminello Zagara Bianca” cultivar in the early ripening stage can be potentially reevaluated as a functional ingredient in botanicals and nutraceutical formulations supporting health care for its occurrence of phenolic and in vivo safety.

AUTHOR CONTRIBUTIONS

Stefania Pagliari: Data curation; investigation. **Mirea Sicari:** Data curation. **Lidia Pansera:** Formal analysis; investigation. **Werther Guidi Nissim:** Validation. **Kamel Mhalhel:** Data curation. **Sepond Rastegar:**

Investigation. **Antonino Germanà**: Methodology. **Nicola Cicero**: Writing—original draft; conceptualization. **Mas-simo Labra**: Conceptualization; writing—original draft; supervision. **Ciro Cannavacciuolo**: Software; formal analysis; writing—original draft. **Giuseppe Montalbano**: Writing—original draft; conceptualization; supervision. **Luca Campone**: Supervision; funding acquisition; project administration; conceptualization.

ACKNOWLEDGMENTS

The research group of Milano Bicocca acknowledges the European Union–NextGenerationEU within the National Biodiversity Future Center (NBFC; Project code CN00000033; CUP: F13C22000720007).

CONFLICT OF INTEREST STATEMENT

The authors declare no conflicts of interest.

ORCID

Werther Guidi Nissim  <https://orcid.org/0000-0001-6738-0122>

REFERENCES

- Barry, G. H., Caruso, M., & Gmitter, F. G. (2020). Commercial scion varieties. In M. Talon, M. Caruso, & F. G. Gmitter (Eds.), *The genus citrus* (Vol. 2020, pp. 83–104) Woodhead Publishing. <https://doi.org/10.1016/B978-0-12-812163-4.00005-X>
- Berk, Z. (2016). By-products of the citrus processing industry. In *Citrus fruit processing* (pp. 219–233). Elsevier.
- Burton, M. D., Rytych, J. L., Amin, R., & Johnson, R. W. (2016). Dietary luteolin reduces proinflammatory microglia in the brain of senescent mice. *Rejuvenation Research*, 19(4), 286–292. <https://doi.org/10.1089/rej.2015.1708>
- Bussmann, A. J. C., Zaninelli, T. H., Saraiva-Santos, T., Fattori, V., Guazelli, C. F. S., Bertozzi, M. M., Andrade, K. C., Ferraz, C. R., Camilios-Neto, D., Casella, A. M. B., Casagrande, R., Borghi, S. M., & Verri, W. A. (2022). The flavonoid hesperidin methyl chalcone targets cytokines and oxidative stress to reduce diclofenac-induced acute renal injury: Contribution of the Nrf2 redox-sensitive pathway. *Antioxidants*, 11(7), 1261. <https://doi.org/10.3390/antiox11071261>
- Cannavacciuolo, C., Pagliari, S., Giustra, C. M., Carabetta, S., Guidi Nissim, W., Russo, M., Branduardi, P., Labra, M., & Campone, L. (2023). LC-MS and GC-MS data fusion metabolomics profiling coupled with multivariate analysis for the discrimination of different parts of faustrime fruit and evaluation of their antioxidant activity. *Antioxidants*, 12(3), 565.
- Cassar, S., Adatto, I., Freeman, J. L., Gamse, J. T., Iturria, I., Lawrence, C., Muriana, A., Peterson, R. T., Van Cruchten, S., & Zon, L. I. (2019). Use of zebrafish in drug discovery toxicology. *Chemical Research in Toxicology*, 33(1), 95–118.
- Chakraborty, C., Hsu, C. H., Wen, Z. H., Lin, C. S., & Agoramoorthy, G. (2009). Zebrafish: A complete animal model for in vivo drug discovery and development. *Current Drug Metabolism*, 10(2), 116–124.
- Cirmi, S., Randazzo, B., Russo, C., Musumeci, L., Maugeri, A., Montalbano, G., Guerrera, M. C., Lombardo, G. E., & Levanti, M. (2021). Anti-inflammatory effect of a flavonoid-rich extract of orange juice in adult zebrafish subjected to *Vibrio anguillarum*-induced enteritis. *Natural Product Research*, 35(23), 5350–5353.
- Dananjaya, S., Chandrarathna, H., Nayanaransi, L., Edussuriya, M., Dissanayake, A., Whang, I., & De Zoysa, M. (2020). Pectin purified from pomelo (*Citrus maxima*) peel as a natural hatching agent for fish embryos. *Aquaculture Research*, 51(8), 3109–3118.
- de Souza, A. B. F., de Matos, N. A., de Freitas Castro, T., de Paula Costa, G., Oliveira, L. A. M., Nogueira, K. O. P. C., Ribeiro, I. M. L., Talvani, A., Cangussú, S. D., & de Menezes, R. C. A. (2022). Effects in vitro and in vivo of hesperidin administration in an experimental model of acute lung inflammation. *Free Radical Biology and Medicine*, 180, 253–262.
- Dueñas, M., Martínez-Villaluenga, C., Limón, R. I., Peñas, E., & Frias, J. (2015). Effect of germination and elicitation on phenolic composition and bioactivity of kidney beans. *Food Research International*, 70, 55–63.
- D’Urso, G., Napolitano, A., Cannavacciuolo, C., Masullo, M., & Piacente, S. (2020). Okra fruit: LC-ESI/LTQOrbitrap/MS/MS n based deep insight on polar lipids and specialized metabolites with evaluation of anti-oxidant and anti-hyperglycemic activity. *Food & Function*, 11(9), 7856–7865.
- D’Urso, G., Pizza, C., Piacente, S., & Montoro, P. (2018). Combination of LC–MS based metabolomics and antioxidant activity for evaluation of bioactive compounds in *Fragaria vesca* leaves from Italy. *Journal of Pharmaceutical and Biomedical Analysis*, 150, 233–240. <https://doi.org/10.1016/J.JPBA.2017.12.005>
- El-Sayed, M. A., Al-Gendy, A. A., Hamdan, D. I., & El-Shazly, A. M. (2017). Phytoconstituents, LC-ESI-MS profile, antioxidant and antimicrobial activities of citrus x limon L. Burm. F. cultivar variegated pink lemon. *Journal of Pharmaceutical Sciences and Research*, 9(4), 375.
- El-Zahar, H., Menze, E. T., Handoussa, H., Osman, A. K., El-Shazly, M., Mostafa, N. M., & Swilam, N. (2022). UPLC-PDA-MS/MS profiling and healing activity of polyphenol-rich fraction of *Alhagi maurorum* against oral ulcer in rats. *Plants*, 11(3), 455.
- Fu, Q., Zhang, C., Lin, Z., Sun, H., Liang, Y., Jiang, H., Song, Z., Wang, H., & Chen, S. (2016). Rapid screening and identification of compounds with DNA-binding activity from *Folium Citri Reticulatae* using on-line HPLC–DAD–MSn coupled with a post column fluorescence detection system. *Food Chemistry*, 192, 250–259.
- Galleano, M., Verstraeten, S. V., Oteiza, P. I., & Fraga, C. G. (2010). Antioxidant actions of flavonoids: Thermodynamic and kinetic analysis. *Archives of Biochemistry and Biophysics*, 501(1), 23–30.
- Gao, L., Gou, N., Amakye, W. K., Wu, J., & Ren, J. (2022). Bioactivity guided isolation and identification of phenolic compounds from *Citrus aurantium* L. with anti-colorectal cancer cells activity by UHPLC-Q-TOF/MS. *Current Research in Food Science*, 5, 2251–2260.
- Garcia, L., Deshaies, S., Constantin, T., Garcia, F., & Saucier, C. (2023). Impact of phenolic composition and antioxidant parameters on the ageing potential of Syrah red wines measured by accelerated ageing tests. *Food Chemistry*, 426, 136613. <https://doi.org/10.1016/J.FOODCHEM.2023.136613>
- Garg, S. S., Gupta, J., Sharma, S., & Sahu, D. (2020). An insight into the therapeutic applications of coumarin compounds and

- their mechanisms of action. *European Journal of Pharmaceutical Sciences*, 152, 105424. <https://doi.org/10.1016/j.ejps.2020.105424>
- Gattuso, G., Caristi, C., Gargiulli, C., Bellocco, E., Toscano, G., & Leuzzi, U. (2006). Flavonoid glycosides in bergamot juice (*Citrus bergamia* Risso). *Journal of Agricultural and Food Chemistry*, 54(11), 3929–3935.
- Goh, R. M. V., Ee, K. H., Pua, A., Huang, Y., Liu, S. Q., Lassabliere, B., & Yu, B. (2022). Neutral loss scan in complement with high-resolution MS/MS: Combination of detection methods for flavonoid and limonoid glycosides analysis. *Journal of Mass Spectrometry*, 57(2), e4810.
- Gómez-Mejía, E., Rosales-Conrado, N., León-González, M. E., & Madrid, Y. (2019). Citrus peels waste as a source of value-added compounds: Extraction and quantification of bioactive polyphenols. *Food Chemistry*, 295, 289–299.
- Guardo, M. D., Moretto, M., Moser, M., Catalano, C., Troggio, M., Deng, Z., Cestaro, A., Caruso, M., Distefano, G., Malfa, S. L., Bianco, L., & Gentile, A. (2021). The haplotype-resolved reference genome of lemon (*Citrus limon* L. Burm f.). *Tree Genetics & Genomes*, 17, 46 <https://doi.org/10.1007/s11295-021-01528-5>
- Hamdan, D. I., El-Shiekh, R. A., El-Sayed, M. A., Khalil, H. M., Mousa, M. R., Al-Gendy, A. A., & El-Shazly, A. M. (2020). Phytochemical characterization and anti-inflammatory potential of Egyptian *Murcott mandarin* cultivar waste (stem, leaves and peel). *Food & Function*, 11(9), 8214–8236.
- Hassoun, E., Kariya, C., & Williams, F. E. (2005). Dichloroacetate-induced developmental toxicity and production of reactive oxygen species in zebrafish embryos. *Journal of Biochemical and Molecular Toxicology*, 19(1), 52–58.
- Imeneo, V., Romeo, R., De Bruno, A., & Piscopo, A. (2022). Green-sustainable extraction techniques for the recovery of antioxidant compounds from “citrus Limon” by-products. *Journal of Environmental Science and Health, Part B*, 57(3), 220–232. <https://doi.org/10.1080/03601234.2022.2046993>
- Jing, Y., Wu, X., Jiang, H., & Wang, R. (2020). Nephroprotective effects of eriocitrin via alleviation of oxidative stress and DNA damage against cisplatin-induced renal toxicity. *Turkish Journal of Biochemistry*, 45(4), 381–388.
- Kumar, S., & Pandey, A. K. (2013). Chemistry and biological activities of flavonoids: An overview. *The Scientific World Journal*, 2013, 162750.
- Lam, K. Y., Ling, A. P. K., Koh, R. Y., Wong, Y. P., & Say, Y. H. (2016). A review on medicinal properties of orientin. *Advances in Pharmacological and Pharmaceutical Sciences*, 2016, 4104595.
- Letamendia, A., Quevedo, C., Ibarbia, I., Virto, J. M., Holgado, O., Diez, M., Izpisua Belmonte, J. C., & Callol-Massot, C. (2012). Development and validation of an automated high-throughput system for zebrafish in vivo screenings. *PLoS ONE*, 7(5), e36690.
- Liu, H., Zhao, H., Che, J., & Yao, W. (2022-a). Naringenin protects against hypertension by regulating lipid disorder and oxidative stress in a rat model. *Kidney & Blood Pressure Research*, 47(6), 423–432. <https://doi.org/10.1159/000524172>
- Liu, W., Wu, L., Liu, W., Tian, L., Chen, H., Wu, Z., Wang, N., Liu, X., Qiu, J., Feng, X., Xu, Z., Jiang, X., & Zhao, Q. (2022-b). Design, synthesis and biological evaluation of novel coumarin derivatives as multifunctional ligands for the treatment of Alzheimer's disease. *European Journal of Medicinal Chemistry*, 242, 114689. <https://doi.org/10.1016/j.ejmech.2022.114689>
- Lubinska-Szczygeł, M., Kuczyńska-Łażewska, A., Rutkowska, M., Polkowska, Ż., Katrich, E., & Gorinstein, S. (2023). Determination of the major by-products of *Citrus hystrix* peel and their characteristics in the context of utilization in the industry. *Molecules (Basel, Switzerland)*, 28(6), 2596. <https://doi.org/10.3390/MOLECULES28062596>
- March, R. E., Lewars, E. G., Stadey, C. J., Miao, X.-S., Zhao, X., & Metcalfe, C. D. (2006). A comparison of flavonoid glycosides by electrospray tandem mass spectrometry. *International Journal of Mass Spectrometry*, 248(1–2), 61–85.
- Mcharek, N., & Hanchi, B. (2017). Maturation effects on phenolic constituents, antioxidant activities and LC-MS /MS profiles of lemon (*Citrus limon*) peels. *Journal of Applied Botany and Food Quality*, 90, 1–9. <https://doi.org/10.5073/JABFQ.2017.090.001>
- Mhalhel, K., Sicari, M., Pansera, L., Chen, J., Levanti, M., Diotel, N., Rastegar, S., Germanà, A., & Montalbano, G. (2023). Zebrafish: A model deciphering the impact of flavonoids on neurodegenerative disorders. *Cells*, 12(2), 252.
- Miao, Y., Yang, J., Yun, Y., Sun, J., & Wang, X. (2021). Synthesis and anti-rheumatoid arthritis activities of 3-(4-aminophenyl)-coumarin derivatives. *Journal of Enzyme Inhibition and Medicinal Chemistry*, 36(1), 450–461. <https://doi.org/10.1080/14756366.2021.1873978>
- Montalbano, G., Mania, M., Guerrero, M. C., Laurà, R., Abbate, F., Levanti, M., Maugeri, A., Germanà, A., & Navarra, M. (2019). Effects of a flavonoid-rich extract from *Citrus sinensis* juice on a diet-induced obese zebrafish. *International Journal of Molecular Sciences*, 20(20), 5116.
- Montalbano, G., Maugeri, A., Guerrero, M. C., Miceli, N., Navarra, M., Barreca, D., Cirmi, S., & Germanà, A. (2021-b). A white grape juice extract reduces fat accumulation through the modulation of ghrelin and leptin expression in an in vivo model of overfed zebrafish. *Molecules (Basel, Switzerland)*, 26(4), 1119.
- Montalbano, G., Mhalhel, K., Briglia, M., Levanti, M., Abbate, F., Guerrero, M. C., D'Alessandro, E., Laurà, R., & Germanà, A. (2021-a). Zebrafish and flavonoids: Adjuvants against obesity. *Molecules (Basel, Switzerland)*, 26(10), 3014.
- Mullen, W., Archeveque, M.-A., Edwards, C. A., Matsumoto, H., & Crozier, A. (2008). Bioavailability and metabolism of orange juice flavanones in humans: Impact of a full-fat yogurt. *Journal of Agricultural and Food Chemistry*, 56(23), 11157–11164.
- Najmanova, I., Dosedel, M., Hrdina, R., Anzenbacher, P., Filipisky, T., Riha, M., & Mladenka, P. (2015). Cardiovascular effects of coumarins besides their antioxidant activity. *Current Topics in Medicinal Chemistry*, 15(9), 830–849.
- Organisation for Economic Co-operation and Development (OECD). (2013). Test No. 236: Fish embryo acute toxicity (FET) test. OECD. <https://www.oecd-ilibrary.org/content/publication/9789264203709-en>
- Otifi, A., George, C., Elsayed, A., & Farag, M. A. (2015). Mechanistic evidence of *Passiflora edulis* (*Passifloraceae*) anxiolytic activity in relation to its metabolite fingerprint as revealed via LC-MS and chemometrics. *Food & Function*, 6(12), 3807–3817.
- Pagliari, S., Cannavacciuolo, C., Celano, R., Carabetta, S., Russo, M., Labra, M., & Campone, L. (2022). Valorisation, green extraction development, and metabolomic analysis of wild artichoke by-product using pressurised liquid extraction UPLC–HRMS and multivariate data analysis. *Molecules (Basel, Switzerland)*, 27(21), 7157. <https://doi.org/10.3390/MOLECULES27217157/S1>

- Parcheta, M., Świsłocka, R., Orzechowska, S., Akimowicz, M., Choińska, R., & Lewandowski, W. (2021). Recent developments in effective antioxidants: The structure and antioxidant properties. *Materials*, 14(8), 1984.
- Pereira, O. R., Silva, A. M., Domingues, M. R., & Cardoso, S. M. (2012). Identification of phenolic constituents of *Cytisus multiflorus*. *Food Chemistry*, 131(2), 652–659.
- Procházková, D., Boušová, I., & Wilhelmová, N. (2011). Antioxidant and prooxidant properties of flavonoids. *Fitoterapia*, 82(4), 513–523.
- Santos, S. A., Pinto, P. C., Silvestre, A. J., & Neto, C. P. (2010). Chemical composition and antioxidant activity of phenolic extracts of cork from *Quercus suber* L. *Industrial Crops and Products*, 31(3), 521–526.
- Śliwka-Kaszyńska, M., Anusiewicz, I., & Skurski, P. (2022). The mechanism of a retro-diels-alder fragmentation of luteolin: Theoretical studies supported by electrospray ionization tandem mass spectrometry results. *Molecules (Basel, Switzerland)*, 27(3), 1032.
- Slob, W. (2002). PROAST: Software for dose-response modeling and benchmark dose analysis. RIVM.
- Stegeman, J. J., Goldstone, J. V., & Hahn, M. E. (2010). Perspectives on zebrafish as a model in environmental toxicology. In *Fish physiology* (Vol. 29, pp. 367–439). Elsevier.
- Tripoli, E., La Guardia, M., Giammanco, S., Di Majo, D., & Giammanco, M. (2007). Citrus flavonoids: Molecular structure, biological activity and nutritional properties: A review. *Food Chemistry*, 104(2), 466–479.
- Tuli, H. S., Garg, V. K., Bhushan, S., Uttam, V., Sharma, U., Jain, A., Sak, K., Yadav, V., Lorenzo, J. M., Dhama, K., Behl, T., & Sethi, G. (2023). Natural flavonoids exhibit potent anticancer activity by targeting microRNAs in cancer: A signature step hinting towards clinical perfection. *Translational Oncology*, 27, 101596. <https://doi.org/10.1016/j.tranon.2022.101596>
- Wan, J., Feng, Y., Du, L., Veeraraghavan, V. P., Mohan, S. K., & Guo, S. (2020). Antiatherosclerotic activity of eriocitrin in high-fat-diet-induced atherosclerosis model rats. *Journal of Environmental Pathology, Toxicology and Oncology*, 39(1), 61–75.
- Wang, Z.-P., Zhang, W., Xing, L.-Z., Zhao, Y.-D., Xu, J., & Zhang, Y.-X. (2024). Therapeutic potential of Coumarin-polyphenolic acid hybrids in PD: Inhibition of α -syn aggregation and disaggregation of preformed fibrils, leading to reduced neuronal inclusion formation. *Bioorganic & Medicinal Chemistry Letters*, 99, 129618. <https://doi.org/10.1016/j.bmcl.2024.129618>
- Yang, W., Ye, M., Liu, M., Kong, D., Shi, R., Shi, X., Zhang, K., Wang, Q., & Lantong, Z. (2010). A practical strategy for the characterization of coumarins in Radix Glehniae by liquid chromatography coupled with triple quadrupole-linear ion trap mass spectrometry. *Journal of Chromatography A*, 1217(27), 4587–4600.
- Yao, L., Liu, W., Bashir, M., Nisar, M. F., & Wan, C. C. (2022). Eriocitrin: A review of pharmacological effects. *Biomedicine & Pharmacotherapy*, 154, 113563.
- Yousefzadeh, M. J., Zhu, Y., McGowan, S. J., Angelini, L., Fuhrmann-Stroissnigg, H., Xu, M., Ling, Y. Y., Melos, K. I., Pirtskhalava, T., Inman, C. L., McGuckian, C., Wade, E. A., Kato, J. I., Grassi, D., Wentworth, M., Burd, C. E., Arriaga, E. A., Ladiges, W. L., Tchkonja, T., ... Niedernhofer, L. J. (2018). Fisetin is a senotherapeutic that extends health and lifespan. *EBioMedicine*, 36, 18–28. <https://doi.org/10.1016/j.ebiom.2018.09.015>
- Zhang, J., Xu, Y., Ho, C.-T., Qiu, J.-Q., Qiu, X.-H., Huang, Z.-H., Zhang, L., & Xu, W. (2022). Phytochemical profile of Tibetan native fruit “Medog lemon” and its comparison with other cultivated species in China. *Food Chemistry*, 372, 131255.
- Zhang, Y., Sun, Y., Xi, W., Shen, Y., Qiao, L., Zhong, L., Ye, X., & Zhou, Z. (2014). Phenolic compositions and antioxidant capacities of Chinese wild mandarin (*Citrus reticulata* Blanco) fruits. *Food Chemistry*, 145, 674–680. <https://doi.org/10.1016/J.FOODCHEM.2013.08.012>
- Nieto, G., Fernández-López, J., Pérez-Álvarez, J. A., Peñalver, R., Ros, G., & Viuda-Martos, M. (2021). Valorization of citrus co-products: Recovery of bioactive compounds and application in meat and meat products. *Plants*, 10(6), 1069.

SUPPORTING INFORMATION

Additional supporting information can be found online in the Supporting Information section at the end of this article.